Bendable Energy-Harvesting Module with Organic Photovoltaic, Rechargeable Battery, and a-IGZO TFT Charging Electronics

Tilo Meister, Koichi Ishida, Reza Shabanpour, Bahman K. Boroujeni, Corrado Carta, Frank Ellinger
Technische Universität Dresden
Dresden, Germany

Niko Münzenrieder, Luisa Petti, Giovanni A. Salvatore, Gerhard Tröster
Swiss Federal Institute of Technology Zurich
Zurich, Switzerland

Michael Wagner
Belectric OPV GmbH,
Nuremberg, Germany

Pol Ghesquiere, Stefan Kiefl
Siemens AG
Munich, Germany

Martin Krebs
VARTA Microbattery GmbH
Ellwangen, Germany

***Abstract*—This work presents an innovative bendable module for solar-energy harvesting. The module consists of a mechanically flexible organic photovoltaic device (OPV), a rechargeable battery, and an a-IGZO TFT charge-control circuit. The total thickness of the module is 1.1 mm. We present measurements of hardware implementations and simulations. On this basis, voltage converter schemes based on a charge pump in the flexible a-IGZO TFT technology are explored, to enhance the range of operation of the module, particularly under low-light conditions. All investigations and data are presented with focus on two variants of the energy harvesting module that differ in nominal output voltage and capacity: a 6 V variant with capacity of 14.4 mAh and a 24 V variant with capacity of 5.5 mAh. Under exposure to 1 sun, both can be charged in less than 4 hours.**

Keywords—Flexible charging electronics, OPV, a-IGZO TFT, flexible rechargeable battery, charge pump, modeling

I. Introduction

Compact energy harvesting modules contribute to enabling the widespread deployment of small devices, such as sensor nodes, over open areas or across large structures. The use of bendable energy-harvesting modules, which can be fabricated in a low temperature processes, improves the cost efficiency of the solution and extends its applicability. For example, it would be possible to attach a flexible semi-transparent organic photovoltaic device (OPV) to a curved glass surface.

The solar energy harvesting module presented in this work is a compact stack of thin and bendable components, arranged as shown in Fig. 1. All the components are processed at low temperatures. Light is captured by a 300 µm-thick, bendable OPV with conjugated polymers. Charging electronics in amorphous indium gallium zinc oxide (a-IGZO) thin-film transistor (TFT) technology are in the second layer, under the OPV. This 100 µm-thick layer is also semi-transparent. The module is completed by a 680 µm-thick NiMH rechargeable battery. The total thickness of the module is 1.1 mm.

To broaden the range of operation of the module, we present and analyze DC-DC converter circuits in a-IGZO TFT technology.

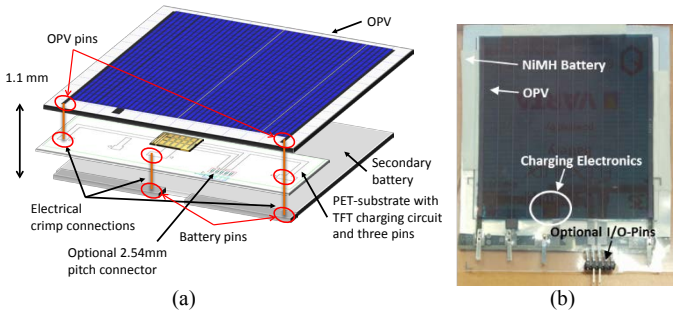

Fig. 1 (a) Three layer stack of the energy harvesting module and (b) top view photo of a 6 V module with the optional I/O-pins.

II. Module For Solar-Energy Harvesting

In this work we consider two variants of the energy harvesting module. The first variant nominally provides 6 V and has a capacity of 14.4 mAh. The second one nominally provides 24 V with a capacity of 5.5 mAh. In the following Sections we first describe the characteristics of the OPV and the rechargeable battery, followed by the a-IGZO TFT technology used, circuit design considerations and measurement results as well as simulation results for the charging electronics.

A. Organic Photovoltaic Device

The OPVs used in this work contain conjugated polymers as active substance. The OPV for the 6 V variant of the energy harvesting module has an active area of 46.1 cm² and an open circuit voltage of V_{oc}=8.3 V. It achieves a very good low-light performance, i.e. its maximum power point is above 6 V down to a light intensity of 100 W/m². Its maximum power point under 1 sun (1 kW/m²) is V_{mpp}=6.3 V / I_{mpp}=24.6 mA. The characteristics of the OPV are shown in Fig. 2 and Table I. The OPV for the 24 V variant of the module exhibits an open circuit voltage V_{oc} of 31.5 V, and a maximum power point of V_{mpp}=24.6 V / I_{mpp}=16.8 mA under 1 sun. The OPVs are the parts with the largest lateral dimensions in the module. The outer dimensions of the batteries and OPVs are concerted such that the OPVs encapsulation extends at least 1.0 cm beyond the batteries in each direction. This extension can be used for mechanical support upon module deployment.

 DOI: 10.1109/ECCTD.2015.7300095.

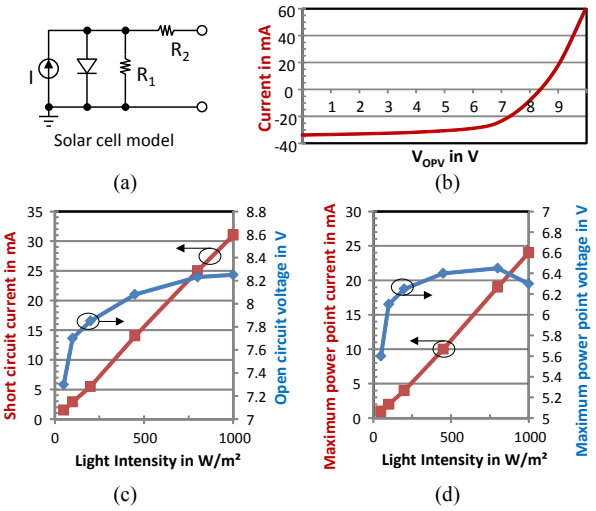

Fig. 2 (a) Electrical solar cell model used for circuit simulations and (b), (c), (d) measured characteristics of the 6 V OPV.

TABLE I. OPV CHARACTERISTICS

OPV	***6V***	***24V***
Outer dimensions OPV package	10 x 10 cm²	14 x 14 cm²
Outer dimensions active region	8 x 8 cm²	12 x 12 cm²
Thickness	300 µm	300 µm
# of cells	11	41
V_{oc}	8.3 V	31.5 V
I_{sc}	38 mA	26 mA

TABLE II. CHARACTERISTICS OF RECHARGEABLE NIMH FLEXIBLE BATTERIES

Rechargeable Battery	***6V***	***24V***
Outer dimensions	9 x 9 cm²	12 x 12 cm²
Thickness	680 µm	680 µm
Capacity	14.4 mAh	5.5 mAh
Maximum voltage	7.2 V	30.0 V
Nominal voltage	6.0 V	24.0 V
End-of-discharge voltage	5.0 V	21.0 V

We use the electrical solar cell model shown in Fig. 2 (a) for the presented simulations. The model parameters were extracted from measurements, which are partly shown in Fig. 2 (b)–(d). These characteristics were measured under a calibrated Oriel solar simulator with Xenon lamp providing 1 sun (AM 1.5, 1 kW/m²) using a source measure unit in combination with a multiplexer system.

B. *Rechargeable NiMH-Battery*

The rechargeable batteries use NiMH chemistry and are matched to the OPVs in size and voltage levels. Both batteries are 680 µm-thick and bendable. Fig. 1 (right) shows the 9 x 9 cm² sized 6 V type under the OPV. The battery characteristics are listed in Table II.

C. *Charging Circuitry on PET Substrate*

A charging circuit is required to reduce the reverse current, see $-I_D$ in Fig. 3 (a), through the OPV, draining the battery, and potentially damaging the OPV under dark conditions. For this purpose, we implemented diode connected FETs (see Subsection 2) in a-IGZO technology and study charge pump circuits (see Subsection 3). The TFT circuits are flip-chip mounted on a PET substrate, as shown in Fig. 3 (b), using a silver particle filled conductive adhesive. The PET substrate also realizes all the lateral interconnections by inkjet-printed silver lines. Vertical interconnections in the stack are made by means of crimps, which at the same time are the externals pins.

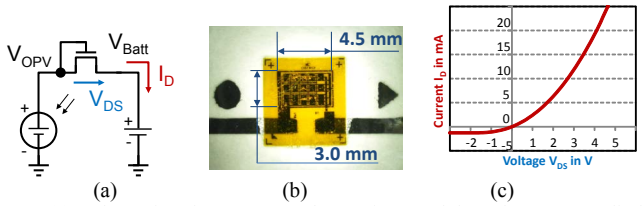

Fig. 3 (a) Schematic of 6 V energy harvesting module, (b) a-IGZO diode connected FET mounted on the PET-substrate with inkjet printed silver interconnect, and (c) measurement results of 6 V diode connected a-IGZO FET.

Optionally, the PET substrate provides I/O-pins, which can be seen in Fig. 1 (b).

1) *a-IGZO TFT Technology*

TFTs receive a justified attention in many fields of applications such as energy harvesting, analog circuits for RFID tags and biomedical sensors. Among the TFT technologies, a-IGZO technologies are currently one of the most promising ones due to the high field-effect mobility of more than 10 cm²/Vs [1]. a-IGZO TFTs can be fabricated using low-temperatures and the resulting devices are bendable down to a radius that depends on the used substrate. Even radii in the order of only 100 µm (diameter of a hair) are possible.

The cross-section of the available a-IGZO TFT is shown in Fig. 4. To cover the requirements regarding voltage breakdown for the 6 V and 24 V variants of the energy harvesting module, the a-IGZO devices in this work are fabricated with different gate oxide thicknesses. A "high-frequency" (HF) type optimizes the TFT device performance for fast switching and allows a supply voltage range of about 3 V to 7 V. The Al_2O_3 gate insulator is 25 nm-thick in this case. Whereas the gate oxide of the "high-voltage" (HV) type is 80 nm-thick and enables operation from a supply voltage of up to 50 V. The more efficient HF type can be used for all electronics of the energy harvesting module variant with nominal supply voltages up to 6 V and for control electronics in both the 6 V and 24 V variants. Circuit parts that require higher voltage tolerances have to be implemented in the HV type.

In practice, low-temperature a-IGZO technologies provide only nMOS TFTs. Compatible pMOS flexible TFTs exist and are based on NiO for example. However, those devices exhibit a mobility of only 0.45 cm²/Vs [2] and are thus prohibitively slower than the a-IGZO based nMOS devices (14.5 cm²/Vs [7]). Only in a high temperature process, NiO based pMOS devices can exhibit a mobility of at most 5.2 cm²/Vs [4].

We use the Rensselaer Polytechnic Institute-amorphous TFT (RPI-aTFT) model template [5] to model a-IGZO TFTs, which enables a fast convergence of transient simulations. The model parameters are extracted from both AC and DC measurements of several HV and HF TFT devices. The HF measurement results can be seen in [6].

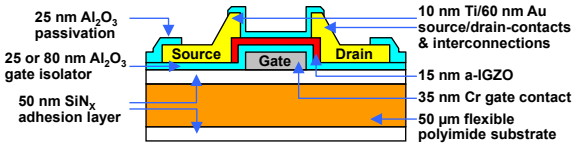

Fig. 4 Cross-section of a-IGZO TFT device [7]. Two variants differing in gate insulator thickness, i.e. 25 nm (high-frequency) and 80 nm (high-voltage), are employed in this work.

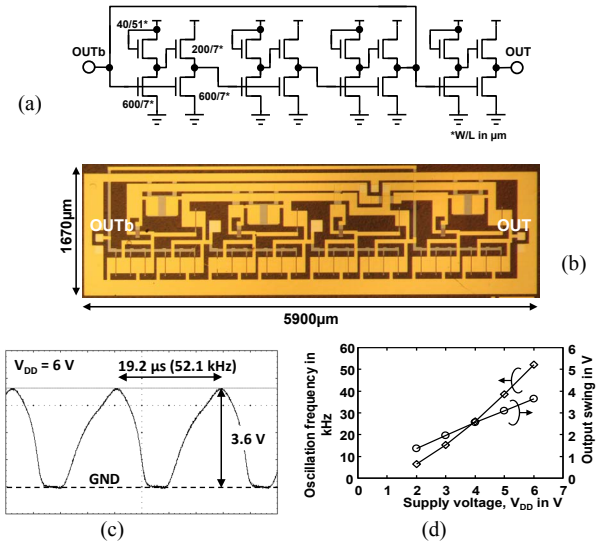

Fig. 5 (a) Schematic and (b) die photo of pCMOS ring oscillator and (c), (d) measurement results of the ring oscillator.

2) Single Diode Connected FET

We implemented diode connected HV FETs as charging electronics. This circuit reduces the reverse current, see $-I_D$ in Fig. 3 (a), through the OPV, which drains the battery, and potentially damages the OPV under dark conditions. The dimensions of the transistors are optimized to enable the full-charge of the batteries within 4 hours under 1 sun, as well as to minimize the reverse current. The channel length and width are 15 µm and 15.75 mm respectively for the 6 V variant; the chip area is 3.0 x 4.5 mm². The 24 V variant has a smaller area of 3.5 x 2.0 mm². It has a channel length of 30 µm and a width of 6.2 mm. The I-V characteristics were measured using a source measure unit. The results for the 6 V variant are shown in Fig. 3 (c). The measured current $I_D \approx -1$ mA at $V_{DS} < 0$ V; for negative voltages V_{DS} is higher than predicted. This is due to inhomogeneities in the specific devices. From the a-IGZO TFT devices used to extract the modelling parameters, it is known that this parameter can be addressed on a technological level. Extrapolating from the a-IGZO transistor devices used for modelling and other previous works, this current can be reduced to as little as $I_D < -10$ uA for $V_{DS} < 0$ [4, 6, 7].

Exposing a 6 V energy harvesting module with a depleted battery (5 V) to 1 sun will result in a charging current of $I_d = 10$ mA, which drops to about 2 mA towards end-of-charge of the battery. Under continued exposure to the sun, diffusion processes in the NiMH battery will prevent further charging and damage to the battery. At the resulting average charging current of about 7 mA and assuming a charging efficiency of 60 % the battery is fully charged after about 3.5 hours.

3) Charge Pump 6 V

Under low-light conditions, e.g. on a clouded winter day or indoors, the output voltage V_{OPV} of the OPV drops and, despite its good low-light performance, can no longer charge the battery. To improve the range of operation of the energy harvesting module, we evaluate and show how a charge pump circuit can be implemented for the energy harvesting module and replace the single diode connected FET.

Previously, organic charge pump circuits have been proposed [8, 9] to generate the relatively large bias voltages

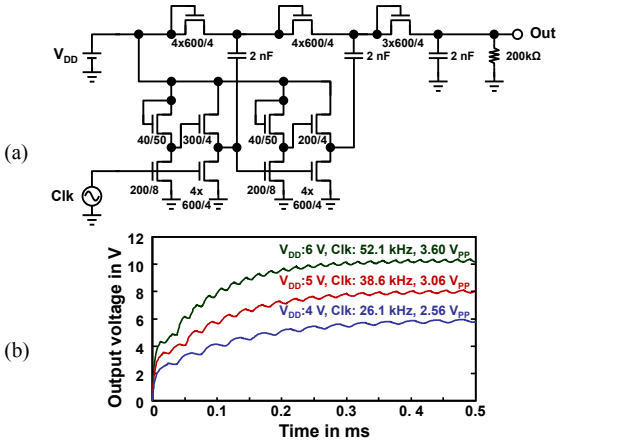

Fig. 6 (a) Schematic and (b) simulation results of the 6 V charge pump, using the measurement results of the pCMOS ring oscillator for clock pulse Clk.

from -40 V to 50 V that are required for many kinds of organic transistors. As it can be seen from these previous works, the optimization of the power efficiency of such circuits is very challenging. The best power efficiency achieved was 48 %, while in other scenarios not even 5% were reached.

The proposed circuit for the 6 V module variant is implemented in the a-IGZO HF type and uses a three-stage pseudo-CMOS [3] (pCMOS) ring-oscillator, which has a wide output swing. Fig. 5 shows the schematic and die photo as well as measurement results, which were acquired on a probe station using an oscilloscope. The complete schematic of the presented charge pump circuit is shown in Fig. 6, including simulation results for three different supply voltages V_{DD} from the OPV. In these simulations, the clock pulse Clk is based on the actual measurement results of the ring-oscillator. A supply voltage V_{DD} of only 4 V results in an output voltage of almost 6 V and allows charging the battery. As can be seen, the output voltage reaches 10 V at V_{DD}=6 V, which has to be considered in an actual application.

4) Charge Pump 24 V

The proposed circuit for the 24 V variant converts the OPV output voltage and allows charging the 24 V battery starting from V_{OPC} of only 17 V. This circuit obviously requires the HV type of the a-IGZO technology (i.e. the thicker gate oxide) and is more challenging to design, because the high-voltage type is optimized for voltage tolerance at the cost of speed.

The charge pump circuit topology is shown in Fig. 7 The required clock signals C and $\overline{C}$ are generated by a five-stage nMOS-inverter ring oscillator that can oscillate across a wide range of supply voltages, while loaded with two modified pCMOS inverters switching currents at nodes V_n and V_p (capacitances C_5, C_6) of the charge pump. The oscillation starts at a solar cell output voltage V_{OPV} of about 5 V. The schematic and transistor dimensions of the ring oscillator are shown in Fig. 8. The oscillation frequency, and voltage swing V_n (ref. Fig. 7) are plotted in Fig. 9 (b).

As described above, the a-IGZO technology only provides nMOS transistors. Therefore, CMOS inverters are unavailable and special techniques are necessary to maximize the voltage swing at nodes V_n and V_p and thus the performance of the charge pump circuit. To maximize the performance we choose a modified pCMOS topology shown in Fig. 10 (a). The

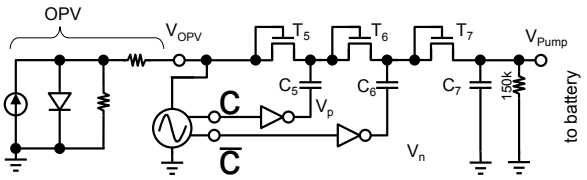

Fig. 7 Schematic of proposed charge pump for the 24 V energy harvesting module (T5=T6=T7: W=4x1mm/L=10um, C_5=C_6=C_7=300pF).

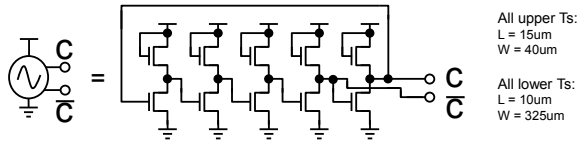

Fig. 8 Five-stage ring oscillator for 24 V module.

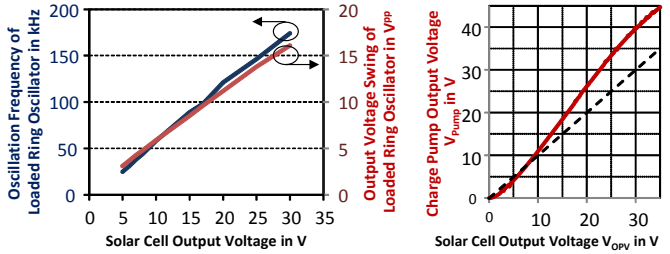

(a) (b)

Fig. 9 (a) Oscillation frequency and output voltage swing (V_n ref. Fig. 10) of five-stage ring oscillator and two pCMOS-inverters while also considering their loads. (b) Output voltage V_{Pump} of charge pump circuit for 24 V module versus OPV voltage V_{OPV}.

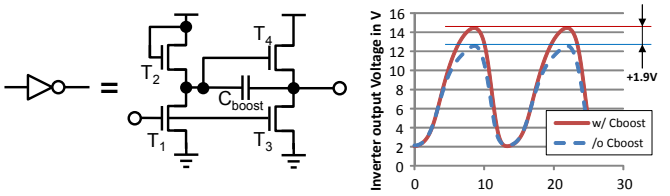

(a) (b)

Fig. 10 (a) Pseudo CMOS inverter with added capacitance C_{boost} and (b) the effect of C_{boost}. Subfigure (b) shows the output voltage swing with and without C_{boost} = 200 pF for a supply voltage of 15 V and an input signal swing at the gate of T1 of 7 V at a frequency of 75 kHz.

pCMOS topology can provide a relatively small inverter input capacitance. This broadens the oscillator's supply voltage range of operation, because the load imposed on the oscillator is relatively small. At the same time the pCMOS topology provides a sufficient driving capability and thus voltage swing at nodes V_n and V_p. To improve the inverter gain within the frequency range (50 kHz to 140 kHz) provided by the ring oscillator across the relevant supply voltages, we add the capacitance C_{boost} to the conventional pCMOS topology, which improves the voltage swing at nodes V_n and V_p (from 12.55 V to 14.45 V at a supply voltage of 15 V). The improvement in output voltage swing of the pCMOS inverter resulting from the introduction of C_{boost} is shown in Fig. 10 (b).

The output voltage of the charge pump V_{Pump} versus V_{OPV} is plotted in Fig. 9 (b). It can be seen that the charge pump circuit converts a V_{OPV} of 17 V to V_{pump} = 21 V. Consequently, any light intensity that results in a voltage V_{OPV} of more than 17 V is sufficient to start charging a depleted battery. The TFT charge pump circuit also prevents reverse current from the battery through the OPV and can replace the diode connected FET presented in Section II-C-2. This effectively reduces the light intensity that is needed by the energy harvesting module to start charging the rechargeable battery. The power consumption of the complete charge pump circuit including the oscillator at V_{OPV}=17 V is 75 mW, while 3 mW are delivered to the output, i.e. the power efficiency $\eta = P_{out}/P_{in}$ of the proposed circuit is 4%. The low efficiency is still acceptable, because the charge pump improves the operation range towards low-light conditions, under which the output voltage of the OPV without the charge pump would not suffice to start charging the battery at all.

III. Conclusion

In this work we presented an innovative 1.1 mm-thick and bendable solar energy harvesting module, with focus on a 6 V variant with 14.4 mAh capacity and a 24 V one with 5.5 mAh capacity. Both can be charged within 4 hours under 1 sun. To improve their range of operation towards low-light conditions we proposed DC-DC converters in a-IGZO TFT technology for both variants of the module. In contrast to previous works on a-IGZO based DC-DC converters [10, 11], we fully integrated the clock signal generation. Whereas, near perfect, non-overlapping external clock signals were assumed by the previous works. Consequently, they were able to achieved better power efficiencies, while we described a much more practical solution. The presented converters enable charging the batteries already with less available light. Therefore the DC-DC converters are beneficial if the energy harvesting module is deployed in a location with mainly low-light conditions, e.g. indoors, where charging without them would be impossible. Under direct sun light, the charging electronics presented in Section II-C-2 are preferable.

Acknowledgment

This work was supported in part by the European Commission under project FLEXIBILITY under Grant 287568 and in part by the German Research Foundation within the Cluster of Excellence "Center for Advancing Electronics Dresden–Organic Path".

References

[1] K. Nomura, et al., "Three-dimensionally stacked flexible integrated circuit: Amorphous oxide/polymer hybrid complementary inverter using n-type a-In-Ga-Zn-O and p-type poly-(9,9-dioctylfluorene-co-bithiophene) thin-film transistors," Appl. Phys. Lett. , vol. 96, no. 26, pp. 263509-1-263509-3, 2010

[2] N.S. Münzenrieder, et al., "Room temperature fabricated flexible NiO/IGZO pn diode under mechanical strain," Solid-State Electronics, vol. 87, pp. 17–20, Sep. 2013

[3] T.-C. Huang, et al., "Pseudo-CMOS: A Design Style for Low-Cost and Robust Flexible Electronics," IEEE Transactions on Electron Devices, vol. 58, no. 1, pp. 141 - 150, Jan. 2011

[4] J. Jiang, et al., "Thermal oxidation of Ni films for p-type thin-film transistors," Physical Chemistry Chemical Physics, no. 15, pp. 6875-6878, 2013.

[5] B. Iniguez, et al., "Universal compact model for longand short-channel Thin-Film Transistors," Solid-State Electronics, vol. 52, pp. 400-405, March 2008

[6] C. Perumal, et al, "A Compact a-IGZO TFT Model Based on MOSFET SPICE Level=3 Template for Analog/RF Circuit Designs," Electron Device Letters, IEEE , vol.34, no.11, pp.1391-1393, Nov. 2013

[7] N. Munzenrieder, et al., "Flexible a-IGZO TFT amplifier fabricated on a free standing polyimide foil operating at 1.2 MHz while bent to a radius of 5 mm," IEEE International Electron Devices Meeting, pp.5.2.1-5.2.4, Dec. 2012

[8] H. Marien, et al., "Organic dual DC-DC upconverter on foil for improved circuit reliability," Electronics Letters, vol.47, no.4, pp.278-280, Feb. 2011

[9] H. Marien, et al., "An organic integrated capacitive DC-DC up-converter", ESSCIRC, pp.510-513, 14-16 Sept. 2010

[10] S. Hong, et al., "DC-DC Converters Using Indium Gallim Zinc Oxide Thin Film Transistors for Mobile Display Applications", Japanese Journal of Applied Physics, vol.49, p.03CB05, 2010

[11] R. Torres, et al., "DC/DC Converter with Transparent Electronics for Application on Photovoltaic Panels", Provas de dissertação do MIEEC, 2013